RING-OPENING PROTONOLYSIS OF SILA[1]FERROCENOPHANES

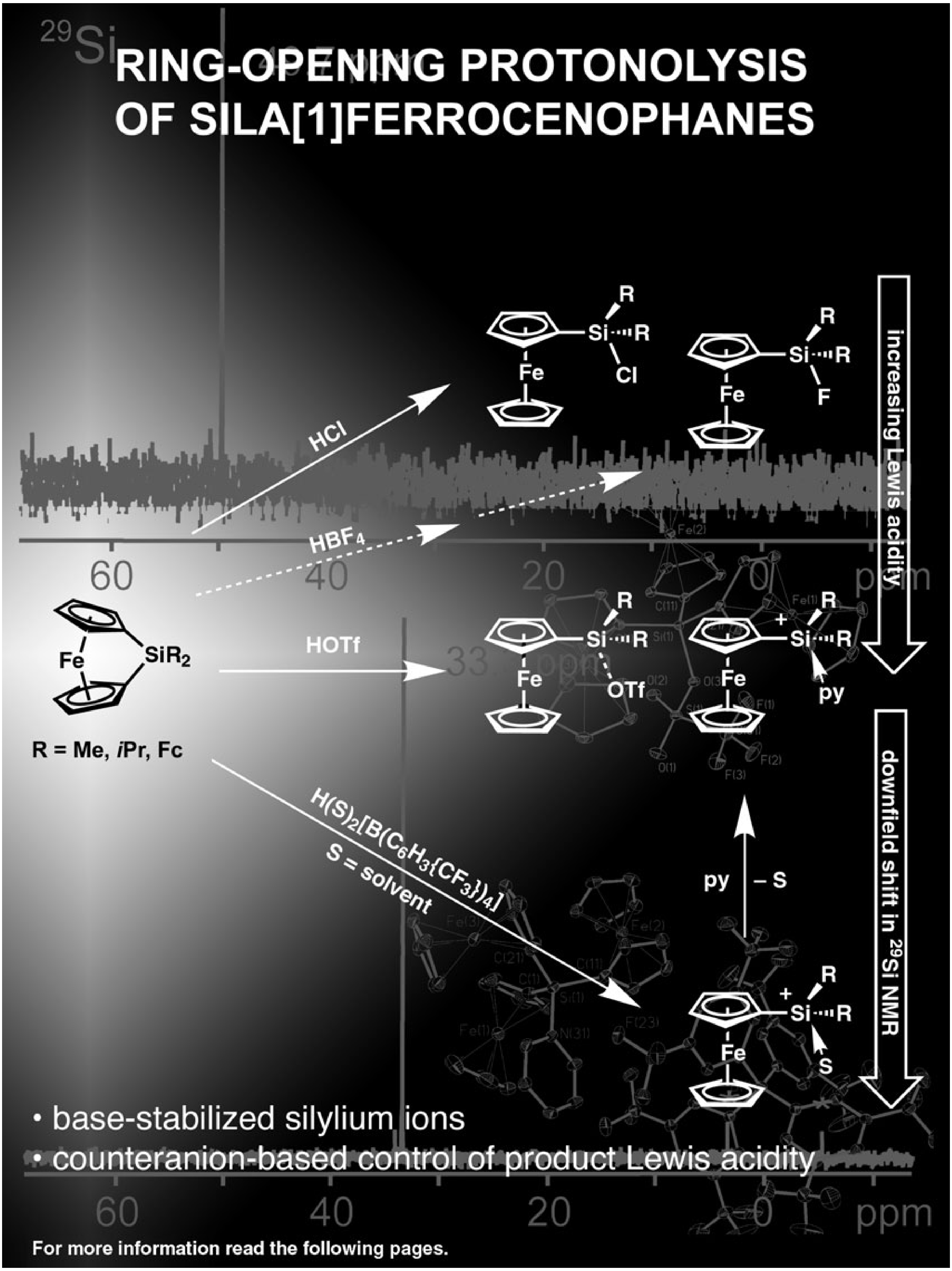

- base-stabilized silylium ions
- counteranion-based control of product Lewis acidity

For more information read the following pages.

DOI: 10.1002/chem.200400859

Ring-Opening Protonolysis of Sila[1]ferrocenophanes as a Route to Stabilized Silylium Ions

Sara C. Bourke,[a] Mark J. MacLachlan,[b] Alan J. Lough,[a] and Ian Manners*[a]

Abstract: The ring-opening reactions of a series of sila[1]ferrocenophanes with protic acids of anions with various degrees of noncoordinating character have been explored. Ferrocenyl-substituted silyl triflates $FcSiMe_2OTf$ (**5a**) and Fc_3SiOTf (**5b**) ($Fc = (\eta^5\text{-}C_5H_4)Fe(\eta^5\text{-}C_5H_5)$) were synthesized by means of HOTf-induced ring-opening protonolysis of strained sila[1]ferrocenophanes $fcSiMe_2$ (**3a**) and $fcSiFc_2$ (**3b**) ($fc = (\eta^5\text{-}C_5H_4)_2Fe$). Reaction of **3a** and **3b** with HBF_4 yielded fluoro-substituted ferrocenylsilanes $FcSiMe_2F$ (**6a**) and Fc_3SiF (**6b**) and suggested the intermediacy of a highly reactive silylium ion capable of abstracting F^- from the $[BF_4]^-$ ion. Generation of the solvated silylium ions $[FcSiMe_2{\cdot}THF]^+$ (**7a**$^+$), $[Fc_3Si{\cdot}THF]^+$ (**7b**$^+$) and $[FcSi\textit{i}Pr_2{\cdot}OEt_2]^+$ (**7c**$^+$) at low temperatures, by reaction of the corresponding sila[1]ferrocenophanes (**3a**, **3b**, and $fcSi\textit{i}Pr_2$ (**3c**), respectively) with $H(OEt_2)(S)TFPB$ ($S = Et_2O$ or THF; TFPB = tetrakis[3,5-bis(trifluoromethyl)phenyl]borate) was monitored by using low-temperature ^1H, ^{13}C, and ^{29}Si NMR spectroscopy. In situ reaction of **7a**$^+$, **7b**$^+$, and **7c**$^+$ with excess pyridine generated $[FcSiMe_2{\cdot}py]^+$ (**8a**$^+$), $[Fc_3Si{\cdot}py]^+$ (**8b**$^+$), and $[FcSi\textit{i}Pr_2{\cdot}py]^+$ (**8c**$^+$), respectively, as observed by ^1H, ^{13}C, and ^{29}Si NMR spectroscopy. A preparative-scale reaction of **3b** with $H(OEt_2)(THF)TFPB$ at −60 °C and subsequent addition of excess pyridine gave isolable red crystals of **8b**-$[TFPB]{\cdot}CHCl_3$, which were characterized by ^1H and ^{29}Si NMR spectroscopy as well as by single-crystal X-ray diffraction.

Keywords: ferrocenophanes · ring-strain · sandwich complexes · silanes · silylium ions

Introduction

Attempts to isolate a free silylium ion $[R_3Si]^+$ in the condensed phase have aroused a great deal of controversy in the literature. The earliest reports of isolation of such species have since been shown to be misleading, and their supposed counterions have been shown to be covalently bound.[1–5] Silylium ions are much more reactive than carbocations, $[R_3C]^+$, as evidenced by the tremendous challenges associated with their isolation, and are generally solvated in the condensed phase. The isolation of species that approach the ideal trigonal-planar geometry have required the use of bulky and/or electron-donating ligands, extremely noncoordinating anions, and inert solvents. Lambert and co-workers have shown that, while abstraction of H^- from Mes_3SiH is not possible due to steric congestion about silicon, $[Mes_3Si]^+$ can be generated through reaction at the exposed end of the allyl group of $Mes_3Si(allyl)$ and is an almost completely isolated cation in the presence of a noncoordinating counterion such as tetrakis(pentafluorophenyl)borate (TPFPB), as evidenced by ^{29}Si NMR spectroscopy ($\delta = 225$ ppm).[6] Unfortunately TPFPB salts are not highly susceptible to crystallization and, until very recently, the closest crystallographically characterized approach to the trigonal-planar environment anticipated for a free silylium ion was provided by the work of Reed and co-workers, and involved the generation of $[\textit{i}Pr_3Si][Br_6CB_{11}H_6]$.[7] It is only through the combined use of the sterically bulky mesityl substituent and a noncoordinating hexahalocarborane anion that isolation and crystallographic characterization of an essentially ideal silylium species, $[Mes_3Si][Br_6CB_{11}Me_6]{\cdot}C_6H_6$, has been achieved.[8,9]

Along with the debate surrounding the isolation of ideal silylium species, a great deal of interest has arisen over coordinated silylium ions, which can still possess a large degree of cationic character associated with the silicon center. This is due to their strong Lewis acidity and potential as highly reactive synthetic reagents, as well as their possible role as

---

[a] S. C. Bourke, Dr. A. J. Lough, Prof. I. Manners
Department of Chemistry, University of Toronto
80 St. George Street, Toronto, ON, M5S 3H6 (Canada)
Fax: (+1) 416-978-6157
E-mail: imanners@chem.utoronto.ca

[b] Prof. M. J. MacLachlan
Current address: Department of Chemistry
University of British Columbia
2036 Main Mall, Vancouver, BC, V6T 1Z1 (Canada)

reactive intermediates in a wide variety of synthetic transformations.[1–3,10] For example, four-coordinate Si cations $[R_3SiL]^+$ (L = neutral donor) have been postulated as be reactive intermediates in the cationic polymerization of hexamethylcyclotrisiloxane, $[Me_2SiO]_3$.[11]

In addition to their reactivity, the ability of such cationic silicon centers to interact with transition metals has garnered much interest. For example, coordination of electron-rich transition-metal fragments has previously been shown to allow the generation of isolable three-coordinate silicon species, for which a silylium ion $[MSiR_2]^+$ can be considered to be a resonance contributor.[12] Interestingly, ferrocenyl moieties have previously been shown to exert a stabilizing influence on adjacent cationic centers, as in the carbocation $FcCPh_2^+$ (**1**) (Fc = $(\eta^5\text{-}C_5H_4)Fe(\eta^5\text{-}C_5H_5)$).[13,14] In crystalline **1**, a tilt of the carbon center towards the electron-rich iron center induces an angle of 20.7° between the plane of the Cp ring and the Cp–CPh_2 bond.[13] In a similar manner, coordination of the iron center from a ferrocenyl moiety might be expected to stabilize a silylium ion. Corey and co-workers synthesized $FcPh_2SiOClO_3$ (**2**) in an effort to generate such a silylium ion but this species was later shown to possess a covalent rather than an ionic structure.[4,5]

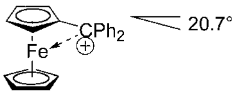

1

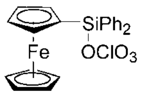

2

The two main routes to the formation of cations with high silylium character are electrophilic abstraction of X^- from four-coordinate R_3SiX molecules (X = for example, Cl, H) and electrophilic addition to, followed by abstraction of, an allyl substituent on silicon.[1,2] The strain inherent in sila[1]ferrocenophanes presents an alternative route to the synthesis of ferrocenyl-substituted silanes and silylium ions. It has recently been shown that ring-opening addition of HCl to the strained Si–C bonds of sila[1]ferrocenophanes (**3**) is a convenient and controlled route to ferrocenylchlorosilanes (**4**) [Eq. (1)].[15] The use of an acid with a noncoordinating anion Y^-, such as tetrakis[3,5-bis(trifluoromethyl)phenyl]borate (TFPB) in the ring-opening addition to sila[1]ferrocenophanes, $fcSiR_2$ (fc = $(\eta^5\text{-}C_5H_4)_2Fe$) might be expected to generate novel coordinated Si cations.[16] Full details of our studies into the use of ring-opening protonolysis to generate novel ferrocenyl-substituted silanes and coordinated silylium ions are reported herein.

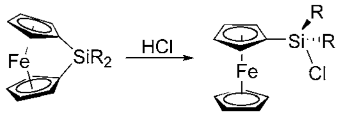

(1)

3 (**a**: R = Me)
(**b**: R = Fc)

4 (**a**: R = Me)
(**b**: R = Fc)

Results and Discussion

Reactions of sila[1]ferrocenophanes with HOTf: To demonstrate the generality of the type of ring-opening protonolysis observed for additions of HCl to sila[1]ferrocenophanes (**3**) [Eq. (1)],[15] we studied the reaction of such strained silacyclic species with a series of acids, whose anions exhibit a range of abilities to coordinate to highly electrophilic cations. As silyl triflates are valuable as functional building blocks for silicon-containing molecules, the reaction of **3** with HOTf was investigated.

Reaction of $fcSiMe_2$ (**3a**) with one equivalent of HOTf at −78 °C in CH_2Cl_2 led to an immediate color change from red to yellow-orange, consistent with ring-opening and the release of strain. Characterization of the reaction mixture by NMR spectroscopy showed conversion to $FcSiMe_2OTf$ (**5a**) [Eq. (2)]. Care was taken not to exceed one equivalent of HOTf, and to thus avoid cleavage of the product's Si–Cp_{ipso} bond; cleavage of Si–C_{aryl} bonds by triflic acid is well known even in the absence of ring strain.[17]

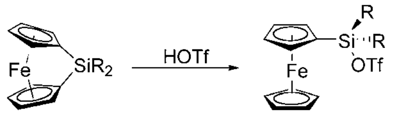

(2)

3 (**a**: R = Me)
(**b**: R = Fc)

5 (**a**: R = Me)
(**b**: R = Fc)

The ^1H NMR spectrum of **5a** (in CD_2Cl_2) showed two pseudo-triplets at $\delta = 4.56$ and 4.27 ppm and a broad singlet at $\delta = 4.24$ ppm that are consistent with the cyclopentadienyl resonances of a ferrocenyl substituent on silicon. The Si-Me resonance at $\delta = 0.74$ ppm was slightly downfield shifted relative to that of the starting material **3a** ($\delta = 0.36$ ppm in C_6D_6).[18]

The ^{29}Si NMR resonance for **5a**, at $\delta = 33.3$ ppm in CD_2Cl_2, is significantly downfield shifted from that of the corresponding strained monomer **3a** (−3.0 ppm in CD_2Cl_2). Notably, it is also downfield shifted, by approximately 10 ppm, from the resonance seen for unstrained $FcSiMe_2Cl$ (**4a**) (22.3 ppm in C_6D_6), derived from the HCl-induced protonolysis of **3a**, and is thus indicative of a significant degree of cationic character on the silicon atom. However, deviation of the ^{29}Si shift of **5a** from the theoretically calculated range for free trialkyl- and triaryl-substituted silylium ions in the condensed phase (>220 ppm)[2] makes it very unlikely that **5a** is fully ionic in nature. Unfortunately, all attempts to grow crystals of **5a** led to isolation of only microcrystalline powders that were unsuitable for study by single crystal X-ray diffraction.

In an analogous manner, reaction of the highly sterically-encumbered sila[1]ferrocenophane $fcSiFc_2$ (**3b**) with HOTf at 0 °C led to generation of Fc_3SiOTf (**5b**) as observed by NMR spectroscopy. The ^1H NMR spectrum shows all three ferrocenyl groups to be equivalent in solution, with pseudo-triplet reasonances for the Si-bound cyclopentadienyl ring at

$\delta = 4.45$ and 4.25 ppm and a resonance attributed to the other cyclopentadienyl fragments at $\delta = 4.09$ ppm. As observed for **5a**, the ^{29}Si NMR resonance for **5b** ($\delta = 18.6$ ppm in the solid state) is significantly downfield from that of the strained monomer **3b** ($\delta = -15.5$ in $CDCl_3$) and downfield shifted by 7.1 ppm from that of Fc_3SiCl (**4b**) ($\delta = 11.5$ ppm), the product of the reaction of **3b** with HCl.

Recrystallization from hexanes allowed the isolation of orange crystals of **5b**. The X-ray crystal structure of **5b** (Figure 1) showed that molecules of this species possess pseudo-tetrahedral geometry around silicon with angles ranging from 102.48(7)° to 114.35(8) (av angle of 109.3°). The reduced steric bulk of the triflate group, relative to that of the ferrocenyl substituents, is accompanied by slightly contracted angles around this substituent (av C-Si-O of 106.0°) and slightly expanded angles between the ferrocenyl substituents (av C-Si-C of 112.7°). The long Si−O bond (1.751(1) Å), compared with an average value of 1.64 Å,[19] suggests a weak covalent interaction between the Fc_3Si moiety and the triflate group. Indeed this bond length is within the longest 1% of all reported Si−O covalent bonds and is very similar to the Si−O bond observed for $Ph_3SiOClO_3$ (1.744(4) Å), which has been shown to be covalent in nature, both in solution and in the solid state.[20] Remarkably, no other examples of a triorgano-subsituted silyl triflates are reported in the Cambridge Structural Database. A somewhat similar structure to that seen for **5b** is found for $(CO)_5Cr{=}Si\mathit{t}Bu_2{\cdot}NaOTf{\cdot}2\,THF$.[21] This complex is represented as a silylene-salt adduct but the silylene fragment could be represented by a transition-metal-substituted silylium fragment that is interacting with the triflate anion. The Si−O bond for this species was found to be 1.857(3) Å, and denotes a significantly weakened interaction between the silylene fragment and the triflate group but is well within the sum of the Van der Waals radii for these atoms. This is similar for other transition-metal-substituted silyl triflates reported in the literature that are thought to have significant silylene character, which would stabilize the electrophilic silicon center and weaken any interaction with the triflate group.[22]

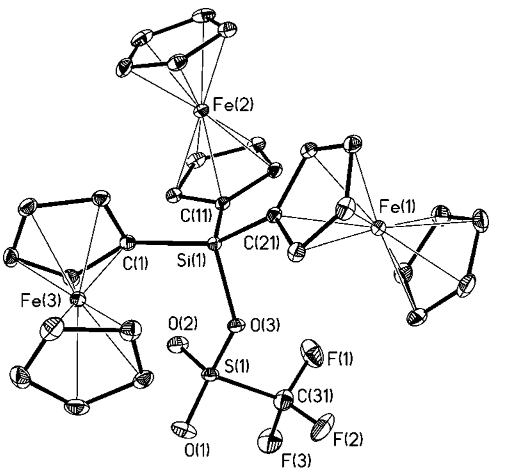

Figure 1. Molecular structure of Fc_3SiOTf (**5b**) with thermal ellipsoids shown at the 30% probability level. Selected bond lengths [Å] and angles [°]: Si(1)−O(3) 1.7506(13), Si(1)−C(1) 1.8344(17), Si(1)−C(11) 1.8286(17), Si(1)−C(21) 1.8275(17); C(1)-Si(1)-O(3) 106.99(7), C(11)-Si(1)-O(3) 108.43(7), C(21)-Si(1)-O(1) 102.48(7), C(1)-Si(1)-C(11) 111.85(8), C(1)-Si(1)-C(21) 111.99(8), C(11)-Si(1)-C(21) 114.35(8).

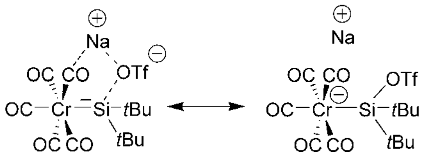

The angle of the Si−C_{ipso} bonds of the ferrocenyl moieties and the corresponding cyclopentadienyl rings all exhibit slight deviations from coplanarity. Thus, two of the ferrocenyl moieties are bent slightly away from the silicon center and have slightly lengthened Si−Fe distances (4.6° and 3.52 Å for Fe(3) and 2.5° and 3.51 Å for Fe(1)), whereas the third group is tilted slightly towards the silicon center (5.5°) with a shortened Si−Fe distance (3.40 Å), despite the resultant increase in congestion around the silicon center. This suggests the possibility that this ferrocenyl moiety may interact electronically with the silicon center, but that any gain in electronic stabilization of the electrophilic silicon center is insufficient to enforce an ionic rather than a covalent interaction between silicon and the triflate group.

The increased reactivity of silyl triflates over analogous silyl halides makes them valuable precursors in organosilicon chemistry.[23] In addition, they are useful as Lewis acid catalysts or initiators for organic transformations.[23,24] The viability of triflic acid induced ring-opening protonolysis of sila[1]ferrocenophanes coupled with the wide variety of available sila[1]ferrocenophanes should provide access to a range of ferrocenyl-substituted silyl triflates with properties that would be tunable through variation of the R groups of **3**.

Reactions of sila[1]ferrocenophanes with HBF_4: The fluorine substituents on the tetrafluoroborate anion make it an even more noncoordinating anion than the triflate anion. Indeed, the proton of the conjugate acid is highly solvated in coordinating solvents such as Et_2O, with the electrophilic proton only electrostatically associated with the anion and coordinated by Et_2O molecules that relieve its electron deficiency. Reaction of **3a** with one equivalent of HBF_4 at −78 °C in CH_2Cl_2 led to isolation of the fluoroferrocenylsilane $FcSiMe_2F$ (**6a**). This effective addition of HF across the Si−C_{ipso} bond of **3a** suggests the presence of a highly reactive cationic silicon intermediate that can extract F^- from the tetrafluoroborate anion (Scheme 1). Such abstraction in the presence of incipient silylium ions is well-precedented for Lewis acid/base adducts such as $[BF_4]^-$.[2]

Similarly, reaction of **3b** with HBF_4 under similar conditions gave rise to the formation of the fluoroferrocenylsilane Fc_3SiF (**6b**). Notably, this reaction was much more susceptible to side reactions such as oxidation and Si−C(Fc) bond

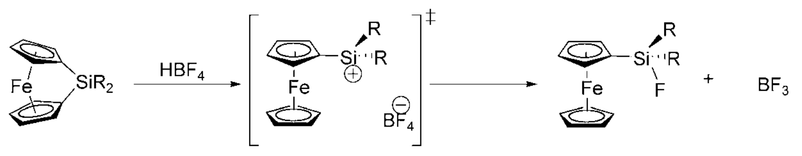

3 (**a**: R = Me)
(**b**: R = Fc)

6 (**a**: R = Me)
(**b**: R = Fc)

Scheme 1. Proposed mechanism for the generation of fluoroferrocenylsilanes **6** from the reaction of HBF_4 with sila[1]ferrocenophanes **3**.

cleavage that ultimately led to a lower yield of **6b**. The increase in oxidation products, indicated by the green color of the reaction mixture, might be attributed to the increase in the number of potential oxidation sites, from one to three, upon moving from the ferrocenyldimethyl system to the triferrocenyl system. In addition, the strong electron-donor behavior of the ferrocenyl groups may make the latter system more susceptible to oxidation. Similarly, with three aromatic $C(sp^2)$–Si bonds, **6b** might be expected to more readily undergo side reactions that involve cleavage of a Si–C(Fc) bond. The alkyl $C(sp^3)$–Si bonds in **6a** seemed to be much more resistant to cleavage under these conditions.

As expected, coupling from the fluorine substituent on silicon to both the ferrocenyl-based *ipso*-carbon atoms of **6a** and **6b**, and the Me substituents of **6a** was evidenced in the ^{13}C NMR spectra of these species, with $^2J_{C,F}$ coupling constants between 17 and 25 Hz. Coupling between the fluorine substituent and the methyl protons of **6a** was also clearly evident in both the ^{1}H and ^{19}F NMR spectra of this species, with clear doublet and septet resonances, respectively, that displayed $^3J_{H,F}$ coupling constants of approximately 7 Hz. The ^{29}Si NMR spectra of **6a** and **6b** showed resonances at $\delta = 23.6$ and 7.6 ppm, respectively, and the one-bond couplings ($^1J_{F,Si}$) to the fluorine substituents were, in both cases, approximately 270 Hz. The shifts of these fluorosilanes are very similar to those previously observed for the analogous chlorosilanes **4a** and **4b**.[15]

It should be noted that care should be taken when performing such reactions to ensure the dryness of the solvent. Although HBF_4 itself is stable in water the product of the proposed fluoride abstraction, BF_3, is quite reactive towards even trace amounts of water and would react to produce HF which could further react with **6** to cleave Si–F bonds. Indeed, the difluoride Fc_2SiF_2 and ferrocene, the logical products of the addition of HF across a Si–C(Fc) bond of **6b** (Scheme 2), have been observed by ^{1}H, ^{13}C, and ^{29}Si NMR spectroscopy when the dryness of the solvent was not ensured in the reaction of **3b** with HBF_4.

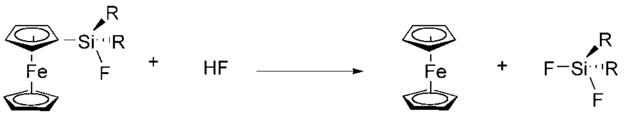

6 (**a**: R = Me)
(**b**: R = Fc)

Scheme 2. Proposed cleavage of Si–C(Fc) bonds of **6** by HF produced by the reaction of BF_3 with trace water impurities.

Although this is, admittedly, a somewhat convoluted route to fluoroferrocenylsilanes it does avoid some of the difficulties associated with the use of HF as a fluoride source as well as provide valuable insight into the mechanism of ring-opening protonolysis. Also, as in the case of triflic acid induced protonolysis, the range of possible fluoroferrocenylsilanes could be potentially controlled through use of the wide variety of available sila[1]ferrocenophanes (**3**).

Reactions of sila[1]ferrocenophanes with $H(OEt_2)(S)$TFPB ($S = OEt_2$ or THF): The postulated generation of a highly reactive silylium ion intermediate in the reaction of sila[1]ferrocenophanes (**3**) with HBF_4 suggested that reaction of **3** with an acid of a noncoordinating ion that is more stable towards degradation than tetrafluoroborate could be expected to allow isolation of the cationic intermediate, and provide a route to ferrocenyl-substituted silylium ions. Highly noncoordinating anions include the hexahalocarboranes, $X_6CB_{11}H_6^-$ (X = Cl, Br, I), and perfluorinated tetraphenylborate (TPFPB).[2,25] The tetrakis[3,5-bis(trifluoromethyl)phenyl]borate (TFPB) anion is less stable to degradation than these examples, as it is prone to fluorine abstraction under some conditions, but is much more stable than the tetrafluoroborate anion ($[BF_4]^-$).[2,25] In addition, literature procedures for the preparation of the acid of this anion, $H(OEt)_2$TFPB, are relatively straightforward.[26] It therefore appeared to be a logical choice for the investigation of this novel pathway.

To investigate whether solvated silicon cations are formed in the reactions of **3** with $H(OEt_2)$(THF)TFPB, we characterized the products by low-temperature NMR spectroscopy. In the reaction of **3a** with $H(OEt_2)$(THF)TFPB at about −60 °C a new ^{29}Si NMR resonance was observed at $\delta = 49.7$ ppm, remarkably downfield from that of **3a** ($\delta = -3.0$ ppm in CD_2Cl_2 at 25 °C).[27,28] The ^{29}Si NMR chemical shift of the product is consistent with similar ether-coordinated silylium species prepared by Sakurai and co-workers[29] (see Table 1) and suggested that the solvated silicon cation **7a**$^+$ was formed at low temperature (Scheme 3). The ^{1}H NMR spectrum at this temperature was consistent with this interpretation and showed sets of peaks assigned to ferrocenyl and $SiMe_2$ groups together with resonances characteristic of free diethyl ether and one set consistent with a coordinated THF molecule. This indicated that the four-coordinate silicon cation **7a**$^+$ had formed. The THF multiplets were shifted downfield ($\delta = 4.35$, 2.15 ppm) relative to the shifts expected for THF in CD_2Cl_2, as would be expected upon coordination to a silicon center with significant cationic character. Some broadening of the coordinated THF reso-

Table 1. ^{29}Si NMR shifts of solvated silylium ions.[a]

Cation	T [°C]	^{29}Si [δ])[b]	Ref
$[Me_3Si(OEt_2)]^+$	−70	66.9	[29]
$[Ph_2MeSi(OEt_2)]^+$	−40	38.0	[29]
$[(2\text{-thienyl})_2MeSi(OEt_2)]^+$	−40	21.4	[29]
7a$^+$ (S=THF)	−60	49.7	this work
8a$^+$	−60	33.3	this work
7b$^+$ (S=THF)	–	–[c]	this work
8b$^+$	25	25.2[d]	this work
7c$^+$ (S=Et_2O)	−80	60.4	this work
8c$^+$	−80	36.2	this work

[a] $[TFPB]^-$ salts. [b] In CD_2Cl_2. [c] No ^{29}Si NMR signal was obtained at low temperature due to the long relaxation time of the Si nucleus and experimental constraints. [d] In $CDCl_3$.

nances was observed, and was possibly indicative of coordinative exchange of the ligand.[29] In the ^{13}C NMR spectrum, corresponding resonances for ferrocenyl and $SiMe_2$ groups, coordinated THF, and free ether molecules were observed. No other species, aside from the expected TFPB anion, were detected in any of the spectra, which indicated clean ring-opening protonolysis of the sila[1]ferrocenophane. After the sample had reached room temperature, it became green, indicative of oxidation to Fe^{III} ferrocenium species.

In a further experiment with **3a**, an aliquot of pyridine (py) was added at −60 °C, after the presence of the silylium ion **7a**$^+$ was confirmed by NMR spectroscopy. Upon addition of the pyridine, the solution changed from yellow to orange and the ^{29}Si NMR resonance moved upfield from $\delta = 49.7$ to 33.3 ppm (Figure 2). This is consistent with what would be expected upon replacement of a weakly coordinated THF molecule with a more strongly coordinated pyridine ligand, which could take up more of the positive charge from the silicon center. This was accompanied by changes to the ^{1}H and ^{13}C NMR spectra that are consistent with the replacement of coordinated THF with pyridine to afford **8a**$^+$ (Figure 3 and Figure 4). In particular, resonances consistent with free THF were observed in place of those for coordinated THF. In this case, when the sample was warmed to 25 °C, the solution remained orange-red for several minutes, which indicated that pyridine stabilizes the cationic species sufficiently to prevent rapid decomposition to an Fe^{III} species at ambient temperature. However, eventual oxidation of room temperature solutions of **8a**$^+$ made isolation of crystals difficult.

Isopropyl substituents, in addition to their steric bulk, have been shown to provide stabilization of electron-deficient silylium centers by means of hyperconjugative stabili-

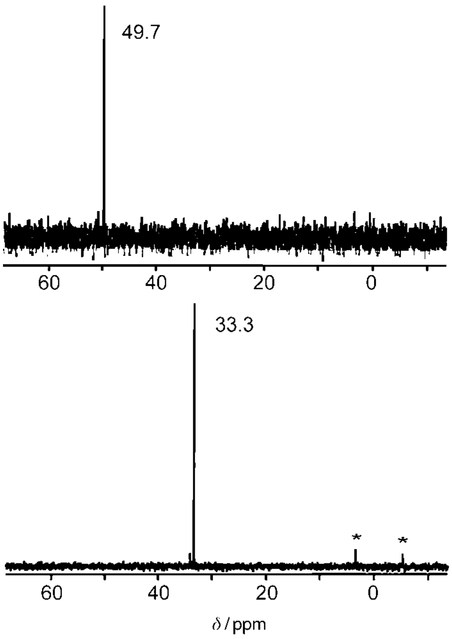

Figure 2. ^{29}Si NMR (in CD_2Cl_2) of in situ generated reaction mixtures containing **7a**$^+$ (top) and **8a**$^+$ (bottom). Peaks marked with * indicate impurities and unreacted monomer **3a**.

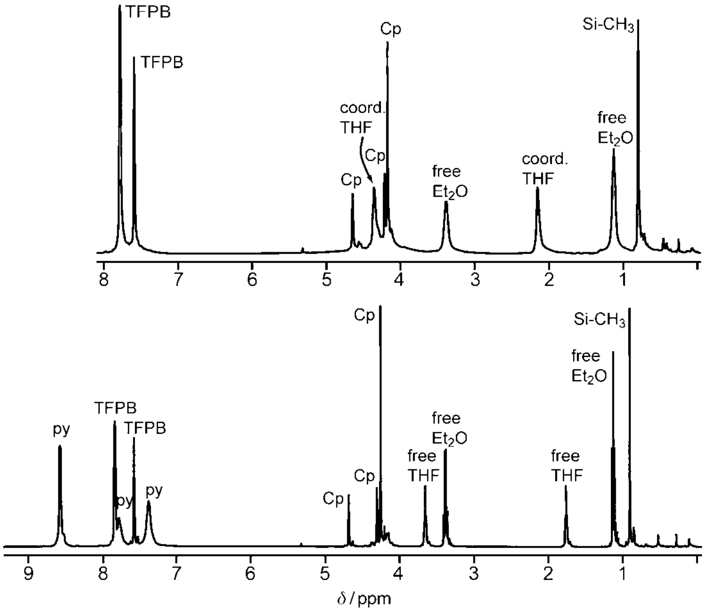

Figure 3. ^{1}H NMR (in CD_2Cl_2) of in situ generated reaction mixtures containing **7a**$^+$ (top) and **8a**$^+$ (bottom).

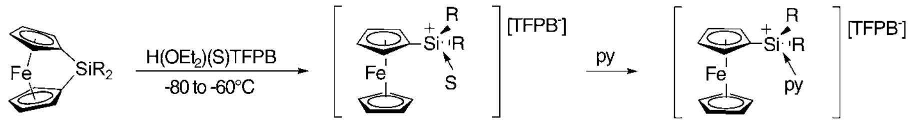

3 **7**$^+$ **8**$^+$

Scheme 3. Reaction between sila[1]ferrocenophanes (**3**) and $[H(OEt_2)(S)][TFPB]$ to yield the base-stabilized ferrocenyl-substituted silylium ion **7**$^+$ and the subsequent displacement of S (THF or Et_2O) by the stronger base pyridine to yield **8**$^+$.

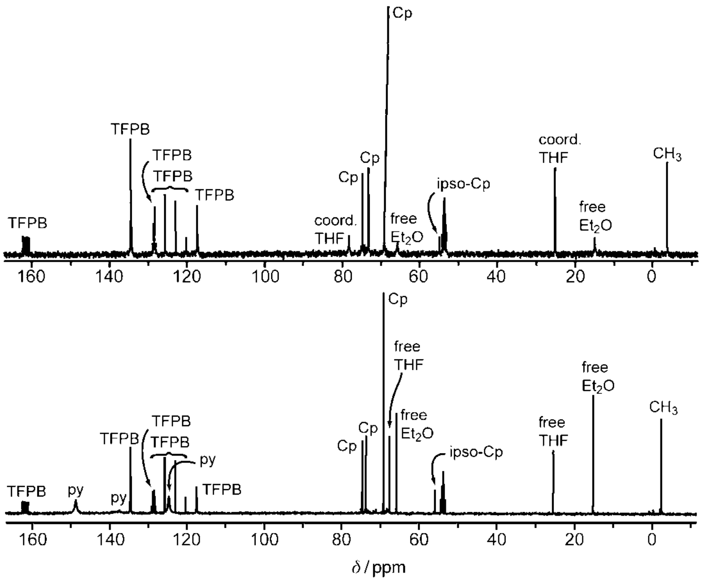

Figure 4. ^{13}C NMR (in CD_2Cl_2) of in situ generated reaction mixtures containing $\mathbf{7a}^+$ (top) and $\mathbf{8a}^+$ (bottom).

zation.[30] To probe the stability of a ferrocenyl-substituted silicon cation in the presence of such stabilizing substituents the synthesis and ring-opening of fcSi*i*Pr$_2$ (**3c**) were undertaken.

Sila[1]ferrocenophane **3c** was synthesized by reaction of dilithioferrocene with diisopropyldichlorosilane at low temperature (−78°C) in Et_2O. The ^{1}H NMR spectrum of **3c** showed, as expected, two pseudo-triplets in the cyclopentadienyl region ($\delta = 4.47$ and 4.11 ppm) as well as heptet and doublet resonances ($\delta = 1.47$ and 1.30 ppm, respectively) attributable to the isopropyl substituents. Single crystals of **3c** were obtained from a low temperature recrystallization and the X-ray crystal structure was determined. The structure of **3c** (Figure 5) shows two independent molecules in the crystal lattice with tilt angles (α) of 19.0° and 19.5°, respectively, for molecules A and B, typical values for strained sila[1]ferrocenophanes.[31]

To monitor the generation of $\mathbf{7c}^+$ at low temperature slight modifications of the experiment used for the generation of $\mathbf{7a}^+$ were required. Species **3c** displays significantly lower solubility in CH_2Cl_2 at low temperature (−80°C) than **3a**. In particular, its kinetic solubility is extremely low and dissolution at low temperature was prohibitively slow. Thus a chilled (−78°C), dilute solution of **3c** in CD_2Cl_2 was added to solid $H(OEt_2)_2$TFPB. An immediate color change from red to yellow was observed as the acid dissolved into solution. The chilled solution was transferred directly to the pre-cooled NMR cavity (−80°C) and ^{1}H, ^{13}C, ^{19}F, and ^{29}Si spectra indicated that generation of $\mathbf{7c}^+$ in solution proceeded at this temperature. The ^{1}H NMR spectrum showed clear evidence for ring-opening protonolysis, with resonances due to the cyclopentadienyl rings at $\delta = 4.65$, 4.29, and 4.20 ppm in a 2:2:5 ratio. Evidence for coordination of Et_2O to the highly electrophlic Si^+ center was seen, with resonances at $\delta = 3.94$ and 1.63 ppm, significantly downfield shifted relative to the corresponding resonances observed for uncoordinated Et_2O ($\delta = 3.39$ and 1.17 ppm, respectively). Resonances in the isopropyl region of the spectrum were complex due to a combination of the diastereotopic nature of the isopropyl methyl groups and restricted rotation of the bulky isopropyl groups. The ^{29}Si NMR showed a resonance for $\mathbf{7c}^+$ at $\delta = 60.4$ ppm which is downfield shifted from that seen for **3c** ($\delta = 5.2$ ppm) by more than 55 ppm. The extent of this difference can be partially explained by the presence of Et_2O, rather than the more basic THF, as the molecule that is stabilizing the electrophilic silicon center.

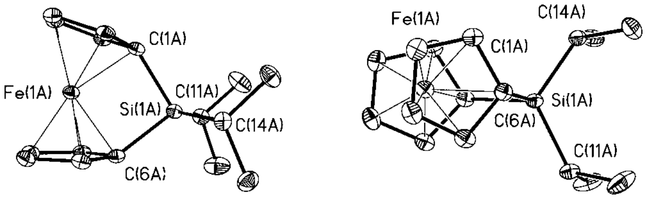

Figure 5. Two views of the molecular structure of one of the independent molecules (A) of **3c** with thermal ellipsoids at 30% probability. Selected bond lengths [Å] and angles [°] for molecule A: Fe(1A)–Si(1A) 2.7026(6), Si(1A)–C(1A) 1.897(2), Si(1A)–C(6A) 1.892(2), Si(1A)–C(11A) 1.884(2), Si(1A)–C(14A) 1.877(2), C(1A)-Si(1A)-C(6A) 96.32(9), C(1A)-Si(1A)-C(11A) 111.45(9), C(1A)-Si(1A)-C(14A) 110.05(9), C(6A)-Si(1A)-C(11A) 109.92(9), C(6A)-Si(1A)-C(14A) 109.91(9), C(11A)-Si(1A)-C(14A) 117.20(10).

Subsequent in situ reaction of $\mathbf{7c}^+$ with excess pyridine led to displacement of the coordinated Et_2O molecule and generation of $\mathbf{8c}^+$. Loss of Et_2O coordination upon addition of pyridine was readily observable by both ^{1}H and ^{13}C NMR and the appearance of resonances consistent with coordinated pyridine became evident. An upfield shift in the ^{29}Si resonance from $\delta = 60.4$ to 36.2 ppm is observed along with the change in the identity of the stabilizing base from Et_2O to pyridine. Species $\mathbf{8c}^+$ is stable in solution up to about 0°C but all attempts to isolate the pyridine-stabilized product led to decomposition.

Thus, a preparative scale reaction of **3c** with $H(OEt_2)$TFPB that was warmed to room temperature following the low temperature reaction and addition of pyridine led to the isolation of one of the decomposition products, $[3,5\text{-}(CF_3)_2C_6H_3]_3B\cdot py$ (**9**), in almost quantitative yields (Scheme 4). Kira and co-workers have previously speculated that the decomposition pathway of the TFPB anion in the presence of silylium ions is likely to involve radical transfer from the tetraarylborate to the silylium ion followed by decomposition of the tetraaryl radical to its constituent triaryl borane, tris(bis-3,5-trifluromethylphenyl)borane, and an aryl radical that is then subject to fluorine atom abstraction by the silyl radical.[29] It follows that any triarylborane generated by such decomposition would associate with pyridine to give the observed adduct **9**, which was characterized by X-ray diffraction (Figure 6). Despite our success in the isolation of **9**, we were not able to confirm the fate of the silylium ion. Initial spectra of the crude reaction mixture indicated the generation of new ferrocenyl-containing species but

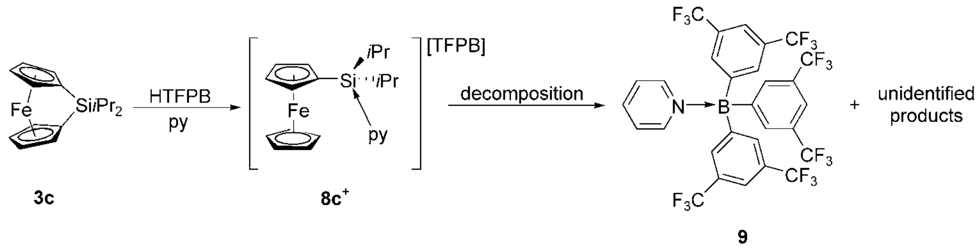

Scheme 4. Generation of $[3,5\text{-}(CF_3)_2C_6H_3]_3B\cdot py$ (**9**) from the decomposition of the pyridine-stabilized silylium ion **8c**-[TFPB]

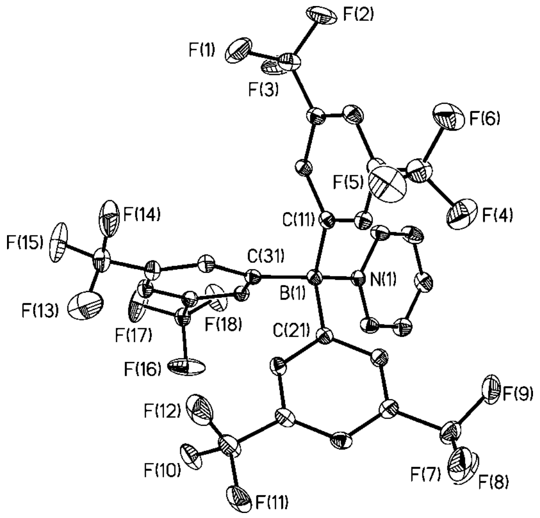

Figure 6. Molecular structure of **9** with thermal ellipsoids at 30% probability. Selected bond lengths [Å] and angles [°]: B(1)–N(1) 1.633(3), B(1)–C(11) 1.637(3), B(1)–C(21) 1.641(3), B(1)–C(31) 1.630(3); N(1)-B(1)-C(11) 108.48(17), N(1)-B(1)-C(21) 107.38(18), N(1)-B(1)-C(31) 108.26(17), C(11)-B(1)-C(21) 110.78(18), C(11)-B(1)-C(31) 111.79(19), C(21)-B(1)-C(31) 109.99(18).

all attempts at isolation of these species proved unsuccessful.

As isolation of crystals of a base-stabilized ferrocenyl-substituted silylium ion was not successful in the presence of methyl or isopropyl substituents we also investigated the reaction of $H(OEt_2)(THF)TFPB$ with the more sterically encumbered sila[1]ferrocenophane **3b**, with two additional bulky ferrocenyl substituents. Although ferrocenyl substituents have been compared to isopropyl substituents with regards to their steric demand they differ significantly in terms of their electronic properties and might be expected to provide additional stabilization to a highly electropositive silicon center. A method identical to that employed for the reaction between **3a** and $H(OEt_2)(THF)TFPB$ was feasible due to the solubility of **3b**, even at low temperatures. The reaction was monitored in situ and results analogous to those seen for **3a** and **3c** were observed by ^1H and ^{13}C NMR spectroscopy. Once again pyridine was added to the cooled sample of $\mathbf{7b}^+$ and a similar change in the shifts of the THF molecules was detected by ^1H NMR and indicated the formation of $\mathbf{8b}^+$. ^{29}Si NMR spectra of both $\mathbf{7b}^+$ and $\mathbf{8b}^+$ were attempted at low temperature but, due to the inability to employ a pulse sequence that makes use of polarization transfer (lack of α-protons) and the apparently long relaxation time of the Si center, no signals were detected.

However, at room temperature, solutions of **8b**-[TFPB] were stable for long periods of time and ^{29}Si NMR characterization was possible. The resonance at $\delta = 25.2$ ppm is more upfield shifted than those observed for $\mathbf{8a}^+$ and $\mathbf{8c}^+$ and indicates a lesser degree of cationic character at the silicon center. The ^1H NMR spectrum obtained for $\mathbf{8b}^+$ at room temperature was consistent with that obtained at $-60\,°C$, with a slight broadening of the pyridine resonances acting as an indication of its reversible coordination in solution. The ^{13}C NMR spectrum, as expected, showed no THF coordination. Both the increased stability of room-temperature solutions of $\mathbf{8b}^+$ and the more shielded ^{29}Si NMR resonance of this species were indicative of greater electronic mediation of the cationic charge at silicon in the presence of three ferrocenyl substituents.

To confirm the structure of **8b**-[TFPB] a single-crystal X-ray diffraction study of crystals obtained from a preparative scale reaction of **3b** with $H(OEt_2)(THF)TFPB$ was undertaken. Crystals were obtained by recrystallization from a mixture of $CHCl_3$ and hexanes at $-50\,°C$. Figure 7 shows the structure of **8b**-[TFPB] in which three ferrocenyl moieties and pyridine are coordinated to the silicon atom. The nearest approach of the anion to the Si atom is 3.93 Å. The Si–N bond length of 1.86 Å is in accord with other silylium-type species coordinated by pyridine, such as $[Me_3Si(py)][X]$ ($X = Br$, I),[32] but longer than the Si–O bond length observed for the crystal structure of Fc_3SiOTf. The Pauling bond order for the interaction between the silicon atom and the nitrogen atom of pyridine was calculated from the bond length to be 0.61,[33] characteristic of a mainly covalent interaction. The sum of the three C-Si-C bond angles in the cation is 337.7°, intermediate between that expected for a trigonal-planar three-coordinate Si cation and a tetrahedral species.

We can see from the structure of **8b**-[TFPB] (Figure 7), as for **5b** (Figure 1), that it is possible that one of the three ferrocenyl substituents is bending back towards the silicon center, allowing its electron-rich iron atom (Fe(2)) to stabilize the cationic Si center. This angular distortion leads to an angle (β) of 7.4(3)° between the plane of the Cp ring and the Si–C(Cp) bond (Figure 7, inset) and the distance between the iron and the silicon center is 3.359(2) Å, versus 3.600(2) Å and 3.644(2) Å for Si(1)–Fe(1) and Si(1)–Fe(3),

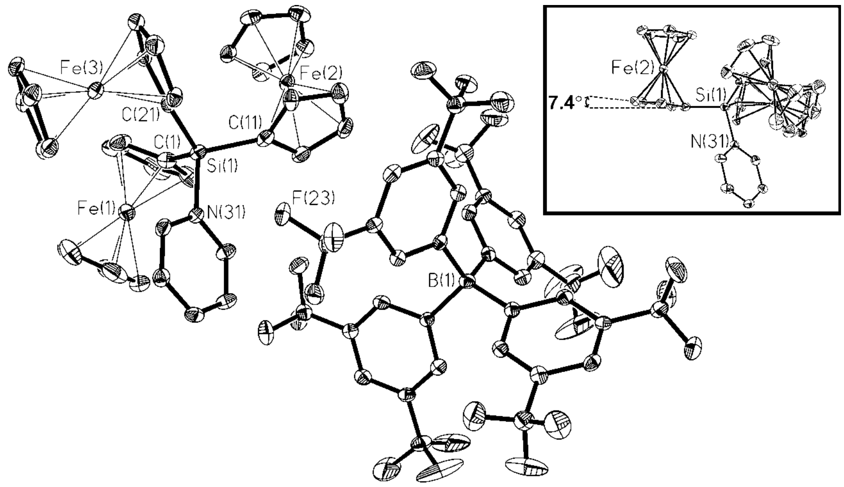

Figure 7. Molecular structure of **8b**-[TFPB] with thermal ellipsoids shown at the 30 % probablility level. Selected bond lengths [Å] and angles [°]: Si(1)–N(31) 1.858(5), Si(1)–C(1) 1.832(6), Si(1)–C(11) 1.833(6), Si(1)–C(21) 1.843(6); C(1)-Si(1)-C(11) 114.9(3), C(1)-Si(1)-C(21) 115.0(3), C(11)-Si(1)-C(21) 107.8(3), C(1)-Si(1)-N(31) 106.8(2), C(11)-Si(1)-N(31) 104.3(2), C(21)-Si(1)-N(31) 107.2(2). The inset shows β angle of 7.4(3)° between the plane of the Cp of the ferrocenyl group (Fe(2)) and the Si–C(Cp_{ipso}) bond.

respectively.[34] Indeed, the other two ferrocenyl substituents are bending away from the silicon center with β angles of 8.7(3)° and 12.4(3)° and show no obvious interaction with the silicon center. Thus, they probably do not provide electronic stabilization through direct Fe···Si interactions in the solid state.

Summary and Conclusions

In summary, we have extended ring-opening protonolysis of sila[1]ferrrocenophanes to acids with anions of moderate and low coordinating ability. This allowed for the synthesis of ferrocenyl-substituted silicon based species FcR_2SiX in which the degree of coordination of X varies form polar covalent (X = OTf) to largely ionic (X = TFPB). Low-temperature NMR studies indicate that addition of $H(OEt_2)(S)TFPB$ (S = THF or Et_2O) to sila[1]ferrocenophanes generates cationic species with silylium character. Structural characterization of **8b**-[TFPB] revealed a cationic silicon center with three ferrocenyl substituents and a coordinating pyridine. The method described should be transferable to other strained silicon-containing heterocycles such as silacyclobutanes, and also to rings containing other Group 14 elements.

Experimental Section

General procedures: Solvents were dried by standard methods, distilled, and stored under nitrogen. Compounds **3a**[28] and **3b**[35] were prepared by standard literature methods. The acid $H(OEt_2)(THF)TFPB$ was prepared by a slight variation of the literature method for the preparation of $H(OEt_2)_2TFPB$.[26] The NaTFPB salt that was used was first recrystallized from THF and was shown by ^1H NMR spectroscopy to possess three THF molecules of crystallization. The product of the subsequent step was shown by ^1H NMR spectroscopy to be $H(OEt_2)(THF)TFPB$ rather than the expected $H(OEt_2)_2TFPB$.

All manipulations involving air- and moisture-sensitive compounds were performed under an atmosphere of prepurified nitrogen using standard Schlenk techniques or in an inert-atmosphere glove box. All solution ^1H, ^{13}C, and ^{29}Si NMR spectra were recorded on Varian Unity 400 or 500 Spectrometers. ^{29}Si NMR spectra were recorded by using either a normal, DEPT, or HMBC pulse sequence and were referenced externally to TMS. Solid-state CP-MAS ^{29}Si NMR spectra were recorded at 39.8 MHz on a Bruker DSX200 spectrometer. All variable-temperature studies were temperature-referenced externally to methanol.

Preparative scale reactions

Reaction of 3a with HOTf; synthesis of $FcSiMe_2OTf$ (5a): A solution of HOTf (35 μL, 0.396 mmol) in CH_2Cl_2 (10 mL) was added slowly to a chilled (−78 °C) solution of **3a** (103 mg, 0.426 mmol) in CH_2Cl_2 (ca. 6 mL). The solution was allowed to warm to room temperature and the solvent was removed under reduced pressure. Extraction of the solid with minimal hexanes and crystallization at −35 °C led to isolation of yellow-orange crystals of $FcSiMe_2OTf$ (**5a**) (91 mg, 59 %). ^1H NMR (CD_2Cl_2, 25 °C): δ = 4.56 (ps t, 2H; Cp), 4.27 (ps t, 2H; Cp), 4.18 (s, 5H; Cp), 0.74 ppm (s, 6H; CH_3); ^{13}C NMR (CD_2Cl_2, 25 °C): δ = 118.9 (q, $^1J_{C,F}$ = 1263 Hz; CF_3) 74.0 (Cp), 73.5 (Cp), 69.4 (Cp), 62.5 (*ipso*-Cp), −0.7 ppm (CH_3); ^{19}F NMR (C_6D_6, 25 °C): δ = −77.4 ppm; ^{29}Si NMR (CD_2Cl_2, 25 °C): δ = 33.3 ppm; MS (70 eV, EI): *m/z* (%): 392 (83) [M^+], 259 (20) [$M-SO_2CF_3$], 243 (68) [$M^+-OSO_2CF_3$], 186 (100) [FcH^+], 121 (27) [$FcH^+-C_5H_5$]; high-resolution MS for $C_{13}H_{15}F_3FeO_3SSi$: calcd 391.981; found 391.981.

Reaction of 3b with HOTf; synthesis of Fc_3SiOTf (5b): A solution of HOTf (29 μL, 0.328 mmol) in CH_2Cl_2 (10 mL) was added to a chilled (0 °C) solution of **3b** (198 mg, 0.349 mmol) in CH_2Cl_2 (25 mL). The solution was allowed to warm to room temperature and the solvent was removed under reduced pressure. The product was extracted with hexanes and recrystallized at −20 °C to give Fc_3SiOTf (**5b**) (31 mg, 13 % yield). ^1H NMR (C_6D_6, 25 °C): δ = 4.45 (ps t, 6H; Cp), 4.25 (ps t, 6H; Cp), 4.09 ppm (s, 15H; Cp); ^{13}C NMR (C_6D_6, 25 °C): δ = 117.9 (CF_3), 74.5 (Cp), 72.3 (Cp), 69.9 (Cp), 63.6 ppm (*ipso*-Cp); ^{19}F NMR (C_6D_6, 25 °C): δ = −77.0 ppm; CP-MAS ^{29}Si NMR (6 kHz): δ = 18.6 ppm; MS (70 eV, EI): *m/z* (%): 732 (100) [M^+], 396 (35) [$M^+-HSO_2CF_3-FcH$], 186 (18) [FcH^+], 121 (10) [$FcH^+-C_5H_5$]; high-resolution MS for $C_{31}H_{27}F_3Fe_3O_3SSi$: calcd 731.945; found 731.945.

Reaction of 3a with HBF_4; synthesis of $FcSiMe_2F$ (6a): A chilled (−78 °C) solution of HBF_4 (55 μL, 54 wt % in Et_2O, 0.399 mmol) in CH_2Cl_2 (5 mL) was added to chilled (−78 °C) solution of **3a** (99 mg, 0.409 mmol) in CH_2Cl_2 (20 mL). The solution was allowed to warm to room temperature and the solvent and volatiles were removed under reduced pressure. The product $FcSiMe_2F$ (**6a**) (39 mg, 37 %) was isolated by sublimation at 50 °C. ^1H NMR (CD_2Cl_2, 25 °C): δ = 4.45 (ps t, 2H; Cp), 4.24 (ps t, 2H; Cp), 4.18 (s, 5H; Cp), 0.49 ppm (d, $^3J_{H,F}$ = 6.9 Hz, 6H; Me); ^{13}C NMR (CD_2Cl_2, 25 °C): δ = 73.6 (Cp), 72.3 (Cp), 69.1 (Cp), 67.2 (d, $^2J_{C,F}$ = 22 Hz, *ipso*-C(Cp)), −0.69 ppm (d, $^2J_{C,F}$ = 17 Hz, Me); ^{19}F NMR (CD_2Cl_2, 25 °C): δ = −150.2 ppm (sep, $^3J_{F,H}$ = 6.8 Hz); ^{29}Si NMR (CD_2Cl_2, 25 °C): δ 23.6 ppm (d, $^1J_{F,Si}$ = 272 Hz); MS (70 eV, EI): *m/z* (%): 262 (100) [M^+], 247 (46) [M^+-Me], 186 (27) [FcH^+], 121 (29) [$FcH^+-C_5H_5$]; high-resolution MS for $C_{12}H_{15}FFeSi$: calcd 262.027; found 262.028.

Reaction of 3b with HBF_4; Fc_3SiF (6b): A chilled (−78 °C) solution of HBF_4 (22 µL, 54 wt % in Et_2O, 0.160 mmol) in CH_2Cl_2 (5 mL) was added to a chilled (−78 °C) solution of **3b** (103 mg, 0.177 mmol) in CH_2Cl_2 (25 mL). The solution was allowed to warm to room temperature and the solvent and volatiles were removed under reduced pressure. The crude product was redissolved in CH_2Cl_2 and filtered to remove oxidized products. Recrystallization from a mixture of CH_2Cl_2 and hexanes yielded Fc_3SiF (**6b**) (25 mg, 26 % yield). ^1H NMR (CD_2Cl_2, 25 °C): $\delta=4.50$ (ps t, 6H; Cp), 4.43 (ps t, 6H; Cp), 4.21 ppm (br s, 15H; Cp); ^{13}C NMR (CD_2Cl_2, 25 °C): $\delta=74.5$ (Cp), 71.9 (Cp), 69.2 (Cp), 66.2 ppm (d, $^2J_{C,F}\sim$ 20 Hz; *ipso*-Cp); ^{19}F NMR (CD_2Cl_2, 25 °C): $\delta=-140.4$ ppm (s); ^{29}Si NMR (CD_2Cl_2, 25 °C): $\delta=7.6$ ppm (d, $^1J_{FSi}=275$ Hz); MS (70 eV, EI): *m/z* (%): 602 (100) [M^+], 351 (34) [$M^+-FcH-C_5H_5$]; high-resolution MS for $C_{30}H_{27}FFe_3Si$: calcd 601.991; found 601.991.

When this reaction was conducted without ensuring the dryness of the CH_2Cl_2 solvent generation of Fc_2SiF_2 and ferrocene as well as **6b** was observed by ^1H, ^{13}C, and ^{29}Si NMR spectroscopy. Fc_2SiF_2: ^1H NMR (CD_2Cl_2, 25 °C): $\delta=4.54$ (ps t, 4H; Cp), 4.42 (ps t, 4H; Cp), 4.28 ppm (br s, 10H; Cp); ^{13}C NMR (CD_2Cl_2, 25 °C): $\delta=73.8$ (Cp), 72.7 (Cp), 69.3 (Cp), 59.7 ppm (t, $^2J_{C,F}\sim$20 Hz; *ipso*-Cp); ^{29}Si NMR (CD_2Cl_2, 25 °C): $\delta=-13.9$ ppm (t, $^1J_{F,Si}=275$ Hz); ferrocene: ^1H NMR (CD_2Cl_2, 25 °C): $\delta=4.21$ ppm; ^{13}C NMR (CD_2Cl_2, 25 °C): $\delta=70.2$ ppm.

Synthesis of fcSi*i*Pr$_2$ (3c): Dichlorodiisopropylsilane (4.5 mL, 25 mmol) was injected slowly to a chilled (−78 °C) suspension of dilithioferrocene·TMEDA adduct (6.181 g, 22.3 mmol) in diethyl ether (ca. 300 mL). The suspension was warmed slowly to room temperature and allowed to react for 3 h. The solvent, TMEDA and excess silane were removed under reduced pressure and the product was redissolved in hexanes. Filtration, to remove LiCl, followed by crystallization at −50 °C, gave red crystals that were purified by sublimation to give fcSi*i*Pr$_2$ (**3c**) (2.273 g, 34 % yield). ^1H NMR (CD_2Cl_2, 25 °C): $\delta=4.48$ (ps t, 4H; Cp), 4.12 (ps t, 4H; Cp), 1.47 (hep, $^3J_{H,H}=7.2$ Hz, 2H; CH), 1.30 ppm (d, $^3J_{H,H}=7.2$ Hz, 12H; CH_3); ^{13}C NMR (CD_2Cl_2, 25 °C): $\delta=77.6$ (Cp), 76.5 (Cp), 34.1 (*ipso*-C(Cp)), 18.4 (CH_3), 12.4 ppm (CH); ^{29}Si NMR (CD_2Cl_2, 25 °C): $\delta=3.2$ ppm. MS (70 eV, EI): *m/z* (%): 298 (100) [M^+], 255 (22) [$M^+-C_3H_7$], 213 (16) [$M^+-2(C_3H_7)+H$]; high-resolution MS for $C_{16}H_{22}FeSi$: calcd 298.084; found 298.084.

Reaction of 3c with $H(OEt_2)_2$TFPB: The solid reagents **3c** (0.042 g, 0.141 mmol) and $H(OEt_2)$(THF)TFPB (0.130 g, 0.129 mmol) were combined in a flask and cooled to −78 °C. Cold (−78 °C) CH_2Cl_2 (ca. 10 mL) was added and the mixture allowed to warm to −40 °C and stirred at this temperature for 10 minutes. Excess pyridine (ca. 0.2 mL) was added and the solution was allowed to warm up to room temperature at which point the solvent was removed under vacuum. A 2:1 $CHCl_3$/hexanes solution of the orange reaction mixture was cooled to −35 °C and yielded clear colourless needles of $[C_6H_3(CF_3)_2]_3B\cdot py$ (**9**) (89 mg, 95 %) that were suitable for characterization by single crystal X-ray diffraction. All attempts to isolate clearly defined product from the orange supernatant were unsuccessful.

9: ^1H NMR (400 MHz, $CDCl_3$, 298 K): $\delta=8.41$ (dd, $^3J_{H,H}=6.8$, $^4J_{H,H}=$ 1.5 Hz, 2H; *o*-py), 8.30 (tt, $^3J_{H,H}=7.6$, $^4J_{H,H}=1.5$ Hz, 1H; *p*-py), 7.81 (dd, $^3J_{H,H}=6.8$, $^3J_{H,H}=7.6$ Hz, 2 H; *m*-py), 7.77 (s, 3 H; BAr-*p*), 7.53 ppm (br, 6 H; BAr-*o*); ^{11}B NMR (96 MHz, $CDCl_3$, 298 K): $\delta=2.80$ ppm (br s); ^{13}C NMR (100 MHz, $CDCl_3$, 298 K): $\delta=151.3$ (br; B-*C*), 147.3 (s; *o*-py), 142.8 (s; *p*-py), 133.6 (br q, $^3J_{C,F}=2$ Hz; BAr-*o*), 130.9 (q, $^2J_{C,F}=33$ Hz; BAr-*m*), 126.8 (s; *m*-py), 123.7 (q, $^1J_{C,F}=272$ Hz; CF_3), 120.8 ppm (sp, $^3J_{C,F}=4$ Hz; BAr-*p*); ^{19}F (282 Hz, $CDCl_3$, 298 K): $\delta=-62.8$ ppm (s; CF_3); elemental analysis calcd (%) for $C_{29}H_{14}BF_{18}N$ (729.219): C 47.77, H 1.94, N 1.92; found: C 47.46, H 1.98, N 1.90.

Unidentified Fc-containing product(s): ^1H NMR (400 MHz, $CDCl_3$, 298 K): $\delta=4.37$ (ps t), 4.31 (ps t), 4.18 (ps t), 4.17 (s), 4.15 (s), 4.11 (ps t)1.25–0.86) (m), 1.11 ppm (s); ^{13}C NMR (100 MHz, $CDCl_3$, 298 K): $\delta=$ 74.3, 73.5, 70.7, 70.2, 68.4, 68.3, 67.9, 18.2–13.1 ppm (m).

Synthesis of [$Fc_3Si\cdot py$][TFPB] (8b-[TFPB]): The solid reagents **3b** (0.230 g, 0.395 mmol) and $H(OEt_2)$(THF)TFPB (0.351 g, 0.347 mmol) were combined in a flask and cooled to −78 °C. Cold (−78 °C) CH_2Cl_2 (ca. 20 mL) was added and the mixture allowed to warm to −60 °C at which point both reagents dissolved to give a yellow-orange mixture. The reaction mixture was stirred at −40 °C for about 10 min and excess pyridine (ca. 0.5 mL) was added causing the solution to turn red. The solution was allowed to warm up to room temperature and the solvent was removed under vacuum. The product was recrystallized from a $CHCl_3$/hexanes mixture at −50 °C to give deep red crystals of **8b**-[TFPB]·$CHCl_3$ (290 mg, 51 % yield). The product was characterized by using ^1H and ^{29}Si NMR spectroscopy as well as single-crystal X-ray diffraction. ^1H NMR (400 MHz, $CDCl_3$, 298 K): $\delta=9.22$ (d, coord. py), 8.23 (t, coord. py), 7.81 (t, coord. py), 7.67 (br, TFPB), 7.46 (br, TFPB), 4.71 (s, 6H; Cp), 4.40 (s, 6H; Cp), 4.06 ppm (s, 15H; Cp); ^{29}Si NMR (79.3 MHz, $CDCl_3$, 298 K): $\delta=25.2$ ppm.

Low-temperature NMR studies

Reaction of 3a with $H(OEt_2)$(THF)TFPB; generation of $7a^+$: The solid reagents **3a** (0.041 g, 0.169 mmol) and $H(OEt_2)$(THF)TFPB (0.141 g, 0.140 mmol) were combined in an NMR tube fitted with a septum. The NMR tube was cooled in liquid nitrogen and 0.5 to 1 mL of CD_2Cl_2 was injected. The frozen sample was placed in the NMR spectrometer and allowed to warm up to −60 °C. The generation of **7a**$^+$ was observed by using ^1H, ^{13}C, and ^{29}Si NMR spectroscopy. ^1H NMR (400 MHz, CD_2Cl_2, 213 K): $\delta=7.78$ (s, 8H; TFPB), 7.59 (s, 4H; TFPB), 4.64 (s, 2H; Cp), 4.35 (br s, 4H; coord. THF), 4.21 (s, 2H; Cp), 4.17 (s, 5H; Cp), 3.39 (q, $^3J_{H,H}=7.18$ Hz, 4H; free Et_2O), 2.15 (br s, 4H; coord. THF), 1.13 (t, $^3J_{H,H}=7.18$ Hz, 6H; free Et_2O), 0.79 ppm (s, 6H; $SiCH_3$); ^{13}C NMR (100 MHz, CD_2Cl_2, 213 K): $\delta=161.7$ (q, $^1J_{B,C}=49.8$ Hz; B-*C*), 134.6 (TFPB-*C*2,6), 128.6 (q, $^2J_{F,C}=31.6$ Hz, TFPB-*C*3,5), 124.4 (q, $^1J_{F,C}=$ 272.6 Hz, TFPB-*C*F_3), 117.4 (s, TFPB-*C*4), 78.4 (coord. THF), 75.0 (Cp), 73.4 (Cp), 69.3 (Cp), 66.0 (free Et_2O), 55.1 (*ipso*-C(Cp)), 25.3 (coord. THF), 15.1 (free Et_2O), −3.5 ppm (Si*C*H_3); ^{29}Si NMR (79.3 MHz, CD_2Cl_2, 213 K): $\delta=49.7$ ppm.

In situ addition of pyridine to $7a^+$; generation of $8a^+$: The NMR tube was briefly removed from the spectrometer and excess pyridine (~0.6 mL) was injected. The conversion of **7a**$^+$ to **8a**$^+$ was observed by using ^1H, ^{13}C, and ^{29}Si NMR. ^1H NMR (400 MHz, CD_2Cl_2, 213 K): $\delta=$ 8.56 (br; py), 7.83 (s, 8H; TFPB), 7.79 (br; py), 7.57 (s, 4H; TFPB), 7.39 (br; py), 4.68 (s, 2H; Cp), 4.29 (s, 2H; Cp), 4.25 (s, 5H; Cp), 3.65 (t, 4H; free THF), 3.37 (q, 4H; free Et_2O), 1.76 (t, 4H; free THF), 1.12 (t, 6H; free Et_2O), 0.90 ppm (s, 6H; $SiCH_3$); ^{13}C NMR (100 MHz, CD_2Cl_2, 213 K): $\delta=161.7$ (q, $^1J_{B,C}=49.8$ Hz; B-*C*), 148.6 (br; py), 137.5 (br; py), 134.5 (TFPB-*C*2,6), 128.6 (q, $^2J_{F,C}=30.1$ Hz; TFPB-*C*3,5), 124.6 (br; py), 124.3 (q, $^1J_{F,C}=272.3$ Hz; TFPB-*C*F_3), 117.4 (s; TFPB-*C*4), 74.6 (Cp), 73.7 (Cp), 69.2 (Cp), 67.7 (free THF), 65.8 (free Et_2O), 55.9 (*ipso*-C(Cp)), 25.4 (free THF), 15.1 (free Et_2O), −2.4 ppm (Si*C*H_3); ^{29}Si NMR (79.3 MHz, CD_2Cl_2, 213 K): $\delta=33.3$ ppm.

Reaction of 3c with $H(OEt_2)_2$TFPB; generation of $7c^+$: A solution of **3c** (0.007 g, 0.023 mmol) in CD_2Cl_2 was injected into a cooled (−78 °C) NMR tube fitted with a septum that contained solid $H(OEt_2)_2$TFPB (0.022 g, 0.023 mmol). The cooled sample was placed in an NMR spectrometer cooled to −80 °C. The generation of **7c**$^+$ was observed by using ^1H,^{13}C, ^{19}F and ^{29}Si NMR spectroscopy. ^1H NMR (400 MHz, CD_2Cl_2, −80 °C): $\delta=7.72$ (s, 8H; TFPB), 7.54 (s, 4H; TFPB), 4.65 (s, 2H; Cp), 4.29 (s, 2H; Cp), 4.20 (s, 5H; Cp), 3.94 (br s, 4H; coord. Et_2O), 3.39 (br, 4H; free Et_2O), 1.63 (br s, 4H; coord. Et_2O), 1.30 (*i*Pr), 1.22 (*i*Pr), 1.17 (br, 6H; free Et_2O), 1.30–0.94 ppm (*i*Pr); ^{13}C NMR (100 MHz, CD_2Cl_2, 213 K): $\delta=161.5$ (q, $^1J_{B,C}=49.0$ Hz; B-*C*), 134.4 (TFPB-*C*2,6), 128.3 (q, $^2J_{F,C}=31.8$ Hz; TFPB-*C*3,5), 124.2 (q, $^1J_{F,C}=272.4$ Hz; TFPB-*C*F_3), 117.3 (s; TFPB-*C*4), 75.0 (coord. Et_2O), 74.0 (Cp), 73.8 (Cp), 69.6 (Cp),66.2 (free Et_2O), 54.4 (*ipso*-Cp), 17.6 (CH_3), 16.8 (coord. Et_2O), 14.7 (free Et_2O), 13.2 ppm (SiCH); ^{19}F NMR (376 MHz, CD_2Cl_2, −80 °C): $\delta=$ −62.4 ppm; ^{29}Si NMR (79.3 MHz, CD_2Cl_2, 213 K): $\delta=60.4$ ppm.

In situ addition of pyridine to $7c^+$; generation of $8c^+$: The NMR tube was briefly removed from the spectrometer and excess pyridine (ca. 5 µL) was injected. The conversion of **7c**$^+$ to **8c**$^+$ was observed by using ^1H, ^{13}C, ^{19}F, and ^{29}Si NMR spectroscopy. ^1H NMR (400 MHz, CD_2Cl_2, 213 K): $\delta=8.51$ (d; py), 7.74 (s, 8H; TFPB), 7.77 (t, py), 7.50 (s, 4H; TFPB), 7.36 (ps t, py), 4.68 (s, 2H; Cp), 4.31 (s, 2H; Cp), 4.25 (s, 5H; Cp), 3.34 (q, 4H; free Et_2O), 1.08 (t, 6H; free Et_2O), 1.17–0.94 (m, 14H; *i*Pr) ppm; ^{13}C NMR (100 MHz, CD_2Cl_2, 213 K) δ 161.6 (q, $^1J_{BC}=49.8$ Hz, B-*C*), 148.0 (br, py), 137.9 (br, py), 134.4 (TFPB-*C*2,6), 128.4 (q, $^2J_{FC}=$

31.6 Hz, TFPB-*C*3,5), 124.4 (br, py), 124.2 (q, $^{1}J_{FC}=272.5$ Hz, TFPB-*C*F$_3$), 117.3 (s, TFPB-*C*4), 74.2 (Cp), 73.8 (Cp), 69.5 (Cp), 65.9 (free Et$_2$O), 54.4 (*ipso*-Cp), 17.3 (CH$_3$), 15.2 (free Et$_2$O), 12.4 (SiCH) ppm; ^{19}F NMR (376 MHz, CD$_2$Cl$_2$, −80 °C) δ −62.4 ppm; ^{29}Si NMR (79.3 MHz, CD$_2$Cl$_2$, −80 °C) δ 36.2 ppm.

Reaction of 3b with H(OEt$_2$)(THF)TFPB; generation of 7b$^+$: Solid **3b** (0.036 g, 0.062 mmol) and H(OEt$_2$)(THF)TFPB (0.053 g, 0.052 mmol) were combined in an NMR tube. The NMR tube was cooled in liquid nitrogen and 0.5 to 1 mL of CD$_2$Cl$_2$ was injected. The frozen sample was placed in the NMR spectrometer and allowed to warm up to −60 °C. The generation of **7b$^+$** was observed by using ^{1}H and ^{13}C NMR spectroscopy. ^{1}H NMR (400 MHz, CD$_2$Cl$_2$, 213 K): δ = 7.75 (s, 8H; TFPB), 7.57 (s, 4H; TFPB), 4.73 (s, 6H; Cp), 4.52 (br , 6H; coord. THF, Cp), 4.21 (s, 15H; Cp), 3.36 (br, 4H; free Et$_2$O), 2.12 (br, 4H; coord. THF), 1.09 ppm (br, 6H; free Et$_2$O); ^{13}C NMR (100 MHz, CD$_2$Cl$_2$, 213 K): δ = 161.6 (q, $^{1}J_{B,C}$ = 49.9 Hz; B-*C*), 134.5 (TFPB-*C*2,6), 128.4 (q, $^{2}J_{F,C}$ = 32.0 Hz, TFPB-*C*3,5), 124.2 (q, $^{1}J_{FC}$ = 273.4 Hz, TFPB-*C*F$_3$), 117.3 (s; TFPB-*C*4), 79.2 (coord. THF), 74.0 (Cp), 73.5 (Cp), 69.4 (Cp), 65.8 (free Et$_2$O), 58.4 (*ipso*-C(Cp)), 25.2 (coord. THF), 15.1 ppm (free Et$_2$O).

In situ addition of pyridine to 7b$^+$; generation of 8b$^+$: The NMR tube was briefly removed from the spectrometer and excess pyridine (ca. 0.6 mL) was injected. The conversion of **7b$^+$** to **8b$^+$** was observed using ^{1}H NMR. ^{1}H NMR (500 MHz, CD$_2$Cl$_2$, 213 K): δ = 9.30 (br, coord. py), 8.68 (br, free py, coord. py), 7.99 (br, coord. py), 7.88 (s, free py) 7.60 (br, TFPB), 7.30 (br, TFPB, free py), 4.68 (s, 6H; Cp), 4.54 (s, 6H; Cp), 4.06 (s, 15H; Cp), 3.62 (br s, free THF), 3.35 (br s, 4H; free Et$_2$O), 1.72 (br s, 4H; free THF), 1.12 ppm (br s, 6H; free Et$_2$O).

X-ray crystallographic data for 3c, 5b, 8b-[TFPB]·CH$_2$Cl$_2$ and 9: *General Procedure:* Selected crystal, data collection, and refinement parameters for **3c**, **5b**·CH$_2$Cl$_2$, **8b**-[TFPB]·CH$_2$Cl$_2$ and **9** are given in Table 2. CCDC-247749 (**3c**), CCDC-247750 (**5b**·CH$_2$Cl$_2$), CCDC-143837 (**8b**-[TFPB]·CH$_2$Cl$_2$) and CCDC-247751 (**9**) contain the supplementary crystallographic data for this paper. These data can be obtained free of charge via www.ccdc.cam.ac.uk/conts/retrieving.html (or from the Cambridge Crystallographic Data Centre, 12 Union Road, Cambridge CB2 1EZ, UK; fax: (+44) 1223-336-033; or email: deposit@ccdc.cam.ac.uk). Single-crystal X-ray diffraction data were collected on a Nonius KappaCCD diffractometer using graphite-monochromated Mo$_{K\alpha}$ radiation (λ = 0.71073 Å). A combination of 1° phi and omega (with kappa offsets) scans were used to collect sufficient data. The data frames were integrated and scaled using the Denzo-SMN package.[36] The SHELXTL/PC V5.1 package was used to solve and refine the structures.[37] Refinement was by full-matrix least-squares on F^2 using all data (negative intensities included). Refinement was optimized with hydrogen atoms in calculated positions. The weighting schemes were $w=1/[\sigma^2(F_o^2)+(0.0334P)^2+1.7196P]$ for **3c**, $w=1/[\sigma^2(F_o^2)+(0.0236P)^2+0.9095P]$ for **5b**·CH$_2$Cl$_2$, $w=1/[\sigma^2(F_o^2)+(0.0658P)^2+11.2754P]$ for **8b**-[TFPB]·CHCl$_3$ and $w=1/[\sigma^2(F_o^2)+(0.0958P)^2+1.6070P]$ for **9** where $P=(F_o^2+2F_c^2)/3$.

Table 2. Summary of crystallographic data for **3c**, **5b**·CH$_2$Cl$_2$, **8b**-[TFPB]·CHCl$_3$ and **9**.

	3c	**5b**·CH$_2$Cl$_2$	**8b**-[TFPB]·CHCl$_3$	**9**
empirical formula	C$_{16}$H$_{22}$FeSi	C$_{32}$H$_{29}$Cl$_2$F$_3$Fe$_3$O$_3$SSi	C$_{68}$H$_{45}$BCl$_3$F$_{24}$Fe$_3$NSi	C$_{29}$H$_{14}$BF$_{18}$N
fw	298.28	817.15	1644.85	729.22
crystal color, habit	orange plate		red plate	colorless plate
temperature [K]	150(1)	150(1)	150(1)	150(1)
wavelength [Å]	0.71073	0.71073	0.71073	0.71073
crystal system	monoclinic	triclinic	triclinic	monoclinic
space group	$P2_1/c$	$P\bar{1}$	$P\bar{1}$	$P2_1/n$
unit cell dimensions				
a [Å]	7.8328(10)	11.109(2)	14.3274(7)	16.6560(3)
b [Å]	17.8452(3)	11.437(2)	14.8789(8)	8.9890(3)
c [Å]	20.9211(3)	12.408(3)	17.3698(9)	19.6400(6)
α [°]	90	95.46(3)	75.701(3)	90
β [°]	91.6060(10)	98.34(3)	85.431(3)	95.8140(18)
γ [°]	90	90.33(3)	68.560(3)	90
volume [Å^3]	2923.2(4)	1552.4(5)	3339.6(3)	2925.39(14)
Z	8	2	2	4
ρ_{calcd} [g cm^{-3}]	1.356	1.748	1.636	1.656
abs coeff [mm^{-1}]	1.094	1.714	0.892	0.177
F(000)	1264	828	1648	1448
crystal size [mm]	0.34 × 0.32 × 0.24	0.35 × 0.30 × 0.29	0.27 × 0.18 × 0.08	0.28 × 0.26 × 0.10
θ range for data collection [°]	$2.60<\theta<27.48$	$2.55<\theta<26.37$	$4.09<\theta<22.50$	$2.58<\theta<27.49$
limiting indices	$-10\le h\le 10$, $-23\le k\le 23$, $-27\le l\le 27$	$-13\le h\le 13$, $-14\le k\le 14$, $-15\le l\le 15$,	$-15\le h\le 15$ $-14\le k\le 16$, $-18\le l\le 18$	$-21\le h\le 21$, $-10\le k\le 11$, $-25\le l\le 25$
reflections collected	23563	27162	32788	24821
independent reflections	6673 (R_{int} = 0.041)	6220		
(R_{int} = 0.030)	8622 (R_{int} = 0.097)	6681 (R_{int} = 0.0515)		
data/restraints/parameters	6673/0/334	6220/3/521	8622/0/910	6681/85/482
goodness of fit on F^2	1.055	1.050	1.026	1.041
final R indices [$I>2\sigma(I)$]				
$R1$	0.0334	0.0236	0.0596	0.0595
$wR2$	0.0811	0.0622	0.1423	0.1568
R indices (all data)				
$R1$	0.0457	0.0255	0.0894	0.0982
$wR2$	0.0885	0.0631	0.1617	0.1845
extinction coefficient	0.0001(6)	0.0045(7)		0.0059(14)
largest diff peak/hole [e Å^{-3}]	0.336/−0.487	0.375/−0.633	0.915/−0.595	0.691/−0.588

Acknowledgement

I.M. would like to acknowledge NSERC for a Discovery Grant and the Canadian Government for a Canada Research Chair. S.C.B. thanks the Ontario Government and the University of Toronto for Fellowships.

---

[1] a) J. B. Lambert, L. Kania, S. Zhang, *Chem. Rev.* **1995**, *95*, 1191–1201; b) J. B. Lambert, S. Zhang, S. M. Ciro, *Organometallics* **1994**, *13*, 2430–2443.

[2] C. A. Reed, *Acc. Chem. Res.* **1998**, *31*, 325–332.

[3] S. Borman, *Chem. Eng. News* **1993**, *71*, 41–42.

[4] a) J. Y. Corey, *J. Am. Chem. Soc.* **1975**, *97*, 3237–3238; b) J. Y. Corey, D. Gust, K. Mislow, *J. Organomet. Chem.* **1975**, *101*, C7-C8.

[5] a) T. J. Barton, A. K. Hovland, C. R. Tully, *J. Am. Chem. Soc.* **1976**, *98*, 5695–5696; b) J. B. Lambert, H. Sun, *J. Am. Chem. Soc.* **1976**, *98*, 5611–5615.

[6] a) J. B. Lambert, Y. Zhao, *Angew. Chem.* **1997**, *109*, 389–391; *Angew. Chem. Int. Ed. Engl.* **1997**, *36*, 400–401; b) J. B. Lambert, Y. Zhao, H. Wu, W. C. Tse, B. Kuhlmann, *J. Am. Chem. Soc.* **1999**, *121*, 5001–5008.

[7] C. A. Reed, Z. Xie, R. Bau, A. Benesi, *Science* **1993**, *262*, 402–404.

[8] a) K.-C. Kim, C. A. Reed, D. W. Elliott, L. J. Mueller, F. Tham, L. Lin, J. B. Lambert, *Science* **2002**, *297*, 825–827; b) P. P. Gaspar, *Science* **2002**, *297*, 785–786.

[9] For some other recent theoretical and synthetic investigations in the area of silylium chemistry see: a) M. Nakamoto, T. Fukawa, A. Sekiguchi, *Chem. Lett.* **2004**, *33*, 38–39; b) A. Sekiguchi, Y. Murakami, N. Fukaya, Y. Kabe, *Chem. Lett.* **2004**, *33*, 530–531; c) T. Okazaki, K. K. Laali, *J. Org. Chem.* **2003**, *68*, 1827–1833; d) J. B. Lambert, L. Lin, S. Keinan, *Org. Biomol. Chem.* **2003**, *1*, 2559–2565; e) R. Meyer, K. Werner, T. Müller, *Chem. Eur. J.* **2002**, *8*, 1163–1172; f) J. Schuppan, B. Herrschaft, T. Müller, *Organometallics* **2001**, *20*, 4584–4592; g) J. B. Lambert, L. Lin, *J. Org. Chem.* **2001**, *66*, 8537–8539; h) T. Nishinaga, Y. Izukawa, K. Komatsu, *J. Am. Chem. Soc.* **2000**, *122*, 9312–9313; i) H. Basch, T. Hoz, S. Hoz, *J. Phys. Chem. A* **1999**, *103*, 6458–6467; j) P. Jutzi, A. Mix, B. Rummel, W. W. Schoeller, B. Neumann, H.-G. Stammler, *Science* **2004**, *305*, 849–851.

[10] For examples of investigation of the catalytic activity of silylium ions see: a) M. Johannsen, K. A. Jørgensen, G. Helmchen, *J. Am. Chem. Soc.* **1998**, *120*, 7637–7638; b) M. Oishi, S. Aratake, H. Yamamoto, *J. Am. Chem. Soc.* **1998**, *120*, 8271–8272.

[11] G. A. Olah, X.-Y. Li, Q. Wang, G. Rasul, G. K. S. Prakash, *J. Am. Chem. Soc.* **1995**, *117*, 8962–8966.

[12] For examples of cationic Si species stabilized by transition metals, see: a) S. K. Grumbine, T. D. Tilley, F. P. Arnold, A. L. Rheingold, *J. Am. Chem. Soc.* **1994**, *116*, 5495–5496; b) D. A. Straus, S. D. Grumbine, T. D. Tilley, *J. Am. Chem. Soc.* **1990**, *112*, 7801–7802.

[13] U. Behrens, *J. Organomet. Chem.* **1979**, *182*, 89–98.

[14] A. A. Koridze, *Russ. Chem. Rev.* **1986**, *55*, 113–126.

[15] a) M. J. MacLachlan, M. Ginzburg, J. Zheng, O. Knöll, A. J. Lough, I. Manners, *New J. Chem.* **1998**, *22*, 1409–1415; b) M. J. MacLachlan, J. Zheng, K. Thieme, A. J. Lough, I. Manners, C. Mordas, R. LeSuer, W. E. Geiger, L. M. Liable-Sands, A. L. Rheingold, *Polyhedron* **2000**, *19*, 275–289.

[16] Preliminary communication: M. J. MacLachlan, S. C. Bourke, A. J. Lough, I. Manners, *J. Am. Chem. Soc.* **2000**, *122*, 2126–2127.

[17] R. Schröck, K. Angermaier, H. Schmidbaur, *Z. Naturforsch. B* **1995**, *50*, 613–618.

[18] D. A. Foucher, R. Ziembinski, B.-Z. Tang, P. M. Macdonald, J. Massey, C. R. Jaeger, G. J. Vancso, I. Manners, *Macromolecules* **1993**, *26*, 2878–2884.

[19] The average value of 1.64 Å is based on a statistical analysis of all of the Si–O covalent bonds described for compounds in the Cambridge Structural Database.

[20] G. K. S. Prakash, S. Keyaniyan, R. Aniszfeld, L. Heiliger, G. A. Olah, R. C. Stevens, H.-K. Choi, R. Bau, *J. Am. Chem. Soc.* **1987**, *109*, 5123–5126.

[21] H. Handwerker, M. Paul, J. Riede, C. Zybill, *J. Organomet. Chem.* **1993**, *459*, 151–156.

[22] See for example: a) D. A. Straus, C. Zhang, G. E. Quimbita, S. D. Grumbine, R. H. Heyn, T. D. Tilley, A. L. Rheingold, S. J. Geib, *J. Am. Chem. Soc.* **1990**, *112*, 2673–2681; b) S. K. Grumbine, D. A. Straus, T. D. Tilley, A. L. Rheingold, *Polyhedron* **1995**, *14*, 127–148.

[23] For reviews on the use of silyl triflates as synthetic precursors see the following reviews and the references contained therein: a) W. Uhlig, *Chem. Ber.* **1996**, *129*, 733–739; b) H. Emde, D. Domsch, H. Feger, U. Frick, A. Götz, H. H. Hergott, K. Hofmann, W. Kober, K. Krägeloh, T. Oesterle, W. Steppan, W. West, G. Simchen, *Synthesis* **1982**, 1–26.

[24] For an example that involves the use of TMSOTf as a cationic initiator for the polymerization of THF see: J. S. Hrkach, K. Matyjaszewski, *Macromolecules* **1990**, *23*, 4042–4046.

[25] J. B. Lambert, L. Kania, S. Zhang, *Chem. Rev.* **1995**, *95*, 1191–1201.

[26] M. Brookhart, B. Grant, A. F. Volpe Jr., *Organometallics* **1992**, *11*, 3920–3922.

[27] D. A. Foucher, B.-Z. Tang, I. Manners, *J. Am. Chem. Soc.* **1992**, *114*, 6246–6248.

[28] A. B. Fischer, J. B. Kinney, R. H. Staley, M. S. Wrighton, *J. Am. Chem. Soc.* **1979**, *101*, 6501–6506.

[29] M. Kira, T. Hino, H. Sakurai, *J. Am. Chem. Soc.* **1992**, *114*, 6697–6700.

[30] Z. Xie, R. Bau, A. Benesi, C. A. Reed, *Organometallics* **1995**, *14*, 3933–3941.

[31] For a recent review on polyferrocenylsilanes see: K. Kulbaba, I. Manners, *Macromol. Rapid Commun.* **2001**, *22*, 711–724.

[32] K. Hensen, T. Zengerly, P. Pickel, G. Klebe, *Angew. Chem.* **1983**, *95*, 739; *Angew. Chem. Int. Ed. Engl.* **1983**, *22*, 725–726.

[33] L. Pauling, *Science* **1994**, *263*, 983–983.

[34] Similar or greater β angles have been observed for several systems that involve ferrocenyl substitution of three- or four-coordinate main group elements such as B and Ge. In most cases direct Fe–heteroelement bonds have been proposed to explain this phenomenon. For example see: a) D. A. Foucher, M. Edwards, R. A. Burrow, A. J. Lough, I. Manners, *Organometallics* **1994**, *13*, 4959–4966; b) B. Wrackmeyer, U. Dörfler, W. Milius, M. Herberhold, *Polyhedron* **1995**, *14*, 1425–1431; c) A. Appel, F. Jäkle, T. Priermeier, R. Schmid, M. Wagner, *Organometallics* **1996**, *15*, 1188–1194; d) M. Scheibitz, J. W. Bats, M. Bolte, H.-W. Lerner, M. Wagner, *Organometallics* **2004**, *23*, 940–942; e) see references [13,14].

[35] M. J. MacLachlan, J. Zheng, K. Thieme, A. J. Lough, I. Manners, C. Mordas, R. LeSuer, W. E. Geiger, L. M. Liable-Sands, A. L. Rheingold, *Polyhedron* **2000**, *19*, 275–289.

[36] Z. Otwinowski, W. Minor, *Methods Enzymol.* **1997**, *276*, 307–326.

[37] G. M. Sheldrick, SHELXTL/PC V5.1, Bruker Analytical X-ray Systems, Madison, WI, 1997.

Received: August 19, 2004